Metallicity of InN and GaN surfaces exposed to NH_3

Weronika Walkosz, Peter Zapol,* and G. Brian Stephenson
Materials Science Division, Argonne National Laboratory, Argonne, Illinois 60439, USA
(Received 9 November 2011; revised manuscript received 20 December 2011; published 23 January 2012)

A systematic study of energies and structures of InN and GaN (0001) surfaces exposed to NH_3 and its decomposition products was performed with first-principles methods. A phenomenological model including electron counting contributions is developed based on calculated DFT energies and is used to identify low-energy structures. These predictions are checked with additional DFT calculations. The equilibrium phase diagrams are found to contain structures that violate the electron counting rule. Densities of states for these structures indicate n-type conductivity, consistent with available experimental results.

DOI: 10.1103/PhysRevB.85.033308 PACS number(s): 68.35.bg, 68.35.Md, 73.20.At

Systematic study of equilibrium surface structures is a prerequisite for understanding the atomic scale mechanisms that occur during crystal growth. GaN and InN growth by metal organic chemical vapor deposition (MOCVD)[1,2] is typically carried out using ammonia (NH_3) to provide the required high nitrogen activity.[3,4] First-principles calculations based on density functional theory (DFT) have been previously used to calculate GaN surface phase diagrams[5–8] under realistic temperatures and pressures typical of MOCVD. In this Brief Report, we report an approach to assess the configurational phase space of InN and GaN surfaces under exposure to NH_3 and its decomposition products, which uses DFT in concert with a phenomenological model to guide the choice of structures. Using this method, we discovered that most of the lowest-energy structures of InN under NH_3 exposure do not obey the electron counting rule (ECR).[9,10] This result has implications for understanding n-type conductivity observed in InN epitaxial films. Previously, the origins of the conductivity were proposed to be related to surface structures,[11] threading dislocations, and point defects.[12–17]

The principles of both semiconductor surface reconstruction[18] and the ECR[9,10] disfavor, but do not forbid, surface terminations with dangling bonds. Such structures are often excluded in first-principles studies based on an intuition-limited subset of possible configurations. Approximately, a hundred distinct structures are possible on NH_x-covered ($x = 0$ to 3) (0001) InN (or GaN) surface considering a relatively small (2×2) surface unit cell. The (2×2) cell is the smallest unit containing a multiple of four surface atoms for which the ECR can be satisfied.[5] To avoid calculating all structures and to provide physical insight, we constructed a phenomenological model based on DFT-calculated energies, analogous to the cluster expansion models applied in the past to metals and alloys.[19–22] Screening of many structures based on this model helped us to identify the most stable surface configurations with a minimal computational cost.

Cluster expansion models for metals involve parameters associated with adsorbate-surface (ϵ_i) and nearest-neighbor adsorbate-absorbate ($\epsilon_{i,j}$) interactions. Since electrons (or holes) due to dangling bonds can be present on a semiconductor surface, we include an additional term for violating the ECR given by $\epsilon_{ECR} = |n|\ u_{\pm}$, where u_+ (u_-) is the energy penalty per electron imposed on a surface having an excess (shortage) of $|n|$ electrons required by the rule. On the polar InN and GaN (0001) surfaces, there are three unpaired electrons per (2×2) unit cell due to the unsaturated In and Ga atoms, respectively. The deviation from the rule n is given by $n = 3 - n_{NH_2} - 2n_{NH} - n_H - 3n_N$, where n_i is the number of adsorbate molecules i per (2×2) area. Structures with $n = 0$ satisfy the ECR and, therefore, do not have dangling bonds. With the binding energy of each structure written as

$$BE_{model} = \sum_i \epsilon_i + \sum_{i,j} \epsilon_{i,j} + \epsilon_{ECR}, \quad (1)$$

the least-squares method was used to find the model parameters that best fit DFT calculated binding energies defined as

$$BE_{DFT} = E_{tot} - E_{bare} - \sum_i n_i \mu_i^{mol}, \quad (2)$$

where E_{tot} is the total energy of a given structure, E_{bare} is the total energy of the relaxed surface with no adsorbates, and μ_i^{mol} is the total energy of an isolated molecule at 0 K.

The DFT computations were performed using the projector augmented wave method as implemented in VASP.[23] For the exchange correlation functional, we used the Perdew-Wang (PW91) parametrization of the generalized gradient approximation (GGA). To obtain accurate band gaps for the optimized lowest-energy structures, density-of-states calculations were performed using the Heyd-Scuseria-Ernzerhof (HSE) hybrid functional.[24] The surfaces were modeled using a supercell approach with periodically repeated slabs of six layers of InN (GaN) and 20 Å of vacuum. The bottom surface of the supercell was passivated with fractionally charged H atoms ($0.75e$), and only the top two layers were allowed to relax. The energy cutoff was set to 400 eV and a $4 \times 4 \times 1$ Monkhorst-Pack grid (24 k points in the irreducible part of Brillouin zone) was used. The shallow In $4d$ (Ga $3d$) electrons were treated as part of the valence shell. The calculated lattice parameters a, c, and the internal parameter u of InN are 3.58 Å, 5.79 Å, and 0.38, and of GaN are 3.22 Å, 5.24 Å, and 0.38, respectively, in agreement with experimental values.[1,25]

Our initial DFT calculations indicated that NH_3 and H bind strongly to the T1 site [see Fig. 1(a)] in agreement with earlier work,[5,6] while N and NH favor the H3 site with empty neighboring T1 sites. NH_2 prefers a bridging position (br) between two surface In (or Ga) atoms if their T1 sites are empty and a different T1 site otherwise. In this work,

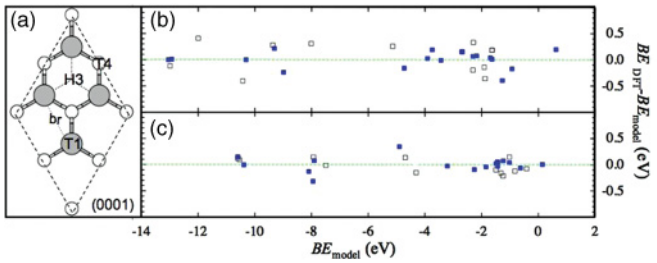

FIG. 1. (Color online) (a) A schematic drawing of a (2 × 2) surface unit cell with different binding sites. The grey circles represent In (Ga) atoms and the white ones represent N. Differences in the binding energies between the structures predicted with the phenomenological model (BE_{model}) and calculated using DFT (BE_{DFT}) plotted against the predicted values for (b) GaN and (c) InN. Configurations used to fit the model parameters and some of those predicted by it are represented by full and empty squares, respectively.

structures involving the T1 sites, which form the largest set of all structures, were treated with the phenomenological model, while those involving the H3 and bridging sites were treated explicitly. DFT energies of sixteen and seventeen structures were used to construct the models for InN and GaN, respectively, with four satisfying the ECR. Comparisons of models for InN with different numbers of parameters have shown that the penalty u_+ for having an excess number of electrons (but not u_-) can be set to zero without changing the quality of the fit. Similarly, interactions of NH_x ($x = 2,3$) with H can be neglected for InN. The latter can be understood in terms of considerably larger lattice parameters of InN, and thus greater distance between two T1 sites, as compared to GaN. Therefore, we used a model with seven parameters for InN structures and with ten parameters for GaN. After determining the model parameters from the initial set of DFT calculations, we used the model to identify all lowest-energy structures, which we then checked by optimizing with DFT.

Figure 1(b) shows the performance of the phenomenological model applied to GaN and InN structures and Table I lists the model parameters. The RMS average deviations of $BE_{\text{model}} - BE_{\text{DFT}}$ for the structures used to determine the model parameters were 0.13 eV and 0.16 eV for InN and GaN, respectively, and were 0.13 and 0.27 eV for the structures not used in the fit. The large deviations observed for GaN may be a result of the phenomenological model not taking into account different possible orientations of the adsorbed species, which has a larger effect for GaN due to its smaller lattice constant.

To compare stabilities of all studied structures, including those with occupied H3 and bridging sites and involving N and NH species, we calculate the Gibbs free energy of formation for each structure[5,6]

$$\Delta G = E_{\text{tot}} - E_{\text{bare}} - \sum_A \mu_A N_A, \quad (3)$$

where N_A is the number of atoms of type A (where A = Ga or In, N, H) in the adsorbates and μ_A is the corresponding chemical potential. Using the conditions $\mu_{\text{In(Ga)}} + \mu_N = \mu^{\text{bulk}}_{\text{InN(GaN)}}$ and $\mu_H = (\mu_{NH_3} - \mu_N)/3$, each surface free energy can be

TABLE I. The parameters of the phenomenological model for binding energy of adsorbates at T1 sites.

Parameter (eV)	InN	GaN
ϵ_{NH_3}	−1.02	−1.95
ϵ_{NH_2}	−3.21	−4.12
ϵ_H	−0.41	−1.14
u_+	0.00	0.11
u_-	1.79	2.67
$\epsilon_{NH_3\text{-}NH_3}$	0.18	0.43
$\epsilon_{NH_3\text{-}NH_2}$	−0.03	0.10
$\epsilon_{NH_3\text{-}H}$	0.00	0.07
$\epsilon_{NH_2\text{-}NH_2}$	0.03	0.04
$\epsilon_{NH_2\text{-}H}$	0.00	0.01

expressed as a function of two parameters, here chosen to be μ_{NH_3} and μ_{In} (μ_{Ga}).[6] The dependence of μ_{NH_3} on the temperature and pressure is given by

$$\mu_{NH_3}(T,p) = \mu^{\text{mol}}_{NH_3} + \tilde{\mu}_{NH_3}(T,p_o) + k_B T \ln[(p/p_o)], \quad (4)$$

where $\tilde{\mu}_{NH_3}(T,p)$ are the contributions from vibrations and rotations of NH_3 as well as the gas entropy at $p_o = 1$ bar, k_B is the Boltzmann constant, T is the temperature, and p is the pressure. While it can be calculated explicitly from DFT, here we use the experimental values for $\tilde{\mu}_{NH_3}(T,p)$.[26] The upper limit for the In (Ga) chemical potential is given by bulk In (Ga), $\mu^{\text{bulk}}_{\text{In}}$ ($\mu^{\text{bulk}}_{\text{Ga}}$), and the lower limit is determined by the enthalpy of formation ΔH_f of InN (GaN). At standard conditions, the experimental values of ΔH_f for InN and GaN are −0.28 and −1.20 eV.[25,27] To correspond to the MOCVD conditions,[3] we extend the lower limit of μ_{In} (μ_{Ga}) to −1.1 eV (−2.2 eV), which gives N activity equivalent to $p_{N_2} \sim 10^7$ bar.

The formation energies of the GaN [see Fig. 2(a)] and InN [see Fig. 2(a)] (0001) surfaces were calculated at T = 0 K and $\mu_{NH_3} = \mu^{\text{mol}}_{NH_3}$. The lowest-energy surface structure

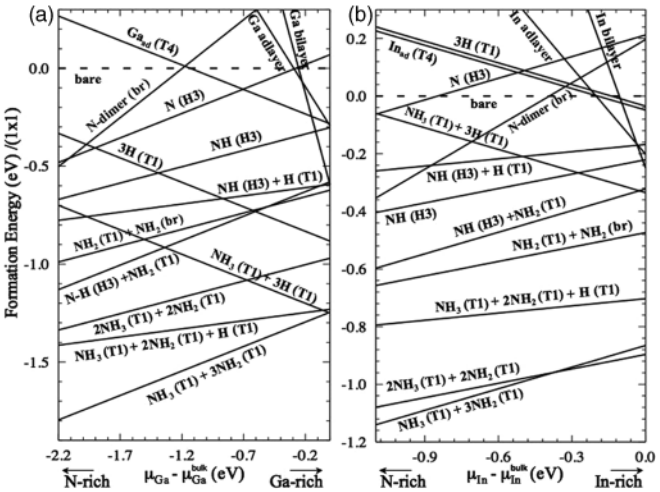

FIG. 2. The T = 0 K formation energies of various configurations on the (a) GaN and (b) InN (0001) surface as a function of the In and Ga chemical potentials, respectively, at $\mu_{NH_3} = \mu^{\text{mol}}_{NH_3}$. The energies are expressed in eV per (1 × 1) cell to include In(Ga) bilayers with a ($\sqrt{3} \times \sqrt{3}$) periodicity.[35] The labels describe the adsorbates and the corresponding binding sites (in parentheses).

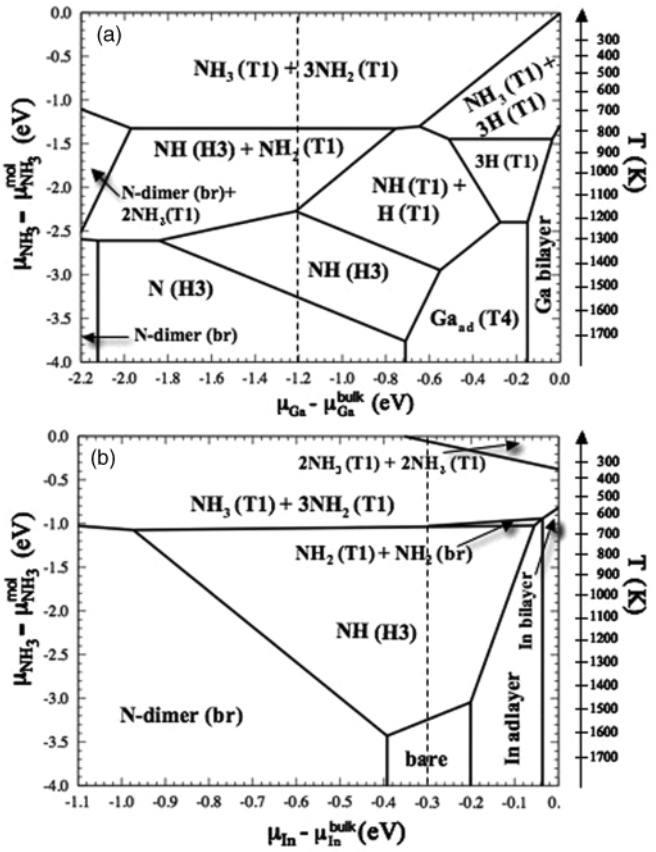

FIG. 3. The calculated phase diagrams of (a) GaN and (b) InN (0001) surfaces as a function of the Ga and In chemical potentials, respectively, and NH_3. The labels describe the adsorbates and their corresponding binding sites (in parentheses). The axis on the right shows temperature corresponding to the NH_3 chemical potential on the phase diagram and pressure of 1 bar. The dashed lines mark the values of enthalpy of formation at standard conditions.

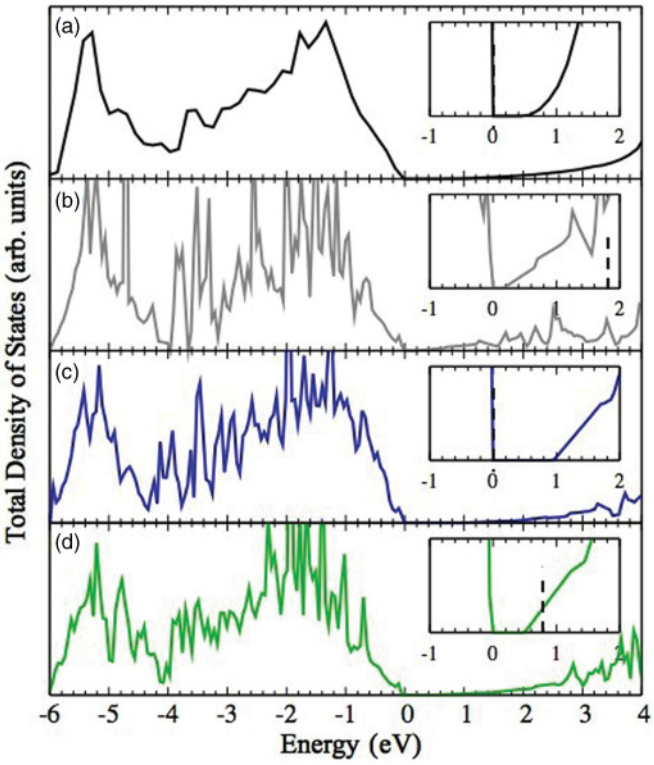

FIG. 4. (Color online) Density of states plots for (a) bulk InN, (b) bare (relaxed) surface, (c) the $NH_3 + 3NH_2$ configuration, and (d) the $2NH_3 + 2NH_2$ configuration, all using HSE functional. The insets show the regions close to the Fermi level (dashed lines) for each structure. The valence-band maxima are aligned at 0 eV.

for GaN over the whole range of μ_{Ga} corresponds to one NH_3 and three NH_2 adsorbed at the T1 sites. This is also the lowest-energy structure at $\mu_H = 1/2\mu_{H_2}^{mol}$, in agreement with previous work.[5,6] Toward the Ga-rich region, a structure with one NH_3 a molecule and three H atoms at the T1 sites becomes energetically competitive.

The formation energy diagram for InN (Fig. 2) is somewhat different from the GaN diagram. In particular, in the In-rich region, the lowest-energy structure for InN consists of $2NH_3$ and $2NH_2$ adsorbates, the structure that is not calculated in the earlier work.[28] Explicit DFT calculation confirms that this structure is 0.02 eV per (1×1) lower in energy than the $NH_3 + 3NH_2$ configuration. Toward the In-poor region, however, the latter starts to dominate. At $\mu_H = 1/2\mu_{H_2}^{mol}$, the difference between the $NH_3 + 3NH_2$ and $2NH_3 + 2NH_2$ structures is 0.12 eV per (1×1) surface unit cell, with the $2NH_3 + 2NH_2$ configuration having the lowest energy over the whole range of μ_{In}.

The phase diagrams of the (0001) surfaces of GaN and InN exposed to NH_3 and its dissociated species as a function of $\mu_{Ga(In)}$ and μ_{NH_3} are shown in Fig. 3. To link the results to growth conditions, a temperature axis showing the dependence of μ_{NH_3} on T for a fixed pressure of 1 bar is also provided. The phase diagram of GaN shows a wide variety of structures as compared to the InN diagram. With the exception of the structure with NH at the H3 site, the GaN phase diagram agrees with the previous work covering the range of μ_{Ga} up to -1.2 eV.[5,6] The NH structure, along with two N-dimer configurations found below -1.2 eV, do not obey the ECR.

Toward the Ga-rich (N-poor) region, structures formed by Ga adsorbates dominate. For InN, with the exception of the $NH_3 + 3NH_2$ structure, all stable configurations do not obey the ECR. It is also interesting to note that toward the NH_3-poor region (at higher T) the bare surface of InN becomes favorable, while for GaN the structure with N at H3 site is more favorable than its bare surface. Towards the metal-rich region, the two phase diagrams also show different structures, with the In-adlayer and Ga adatom configurations present at InN and the GaN surfaces, respectively.

We examined the electronic properties of the most stable structures in the NH_3-rich region by calculating their densities of states (DOS). The DOS of bulk InN, the bare surface, and the $NH_3 + 3NH_2$ and $2NH_3 + 2NH_2$ structures, are shown in Fig. 4 . With this approach, the band gap of bulk InN was found to be 0.59 eV in relatively good agreement with the experimental result of 0.67 ± 0.05 eV.[29,30] It is clear from the figure that while the $NH_3 + 3NH_2$ surface is semiconducting with a band gap of 0.98 eV, both the bare and the $2NH_3 + 2NH_2$ surface structures are conducting. Previous studies[11,31,32] explained conductivity of bare InN surfaces in terms of the narrow band gap of InN and its large electron

affinity, which causes the ECR to be broken. Our estimate of the electron surface accumulation based on the $2NH_3 + 2NH_2$ structure is 0.20 nm^{-2}, which compares well with the reported values of 0.16–0.24 nm^{-2}.[33,34] The results of this study thus provide a different, not structural defect related, explanation for the observed electron accumulation at InN polar surfaces and the propensity for the *n*-type conductivity of the material.

In summary, a complete study of possible structures was performed on the (0001) surfaces of InN and GaN in the presence of NH_3 and its decomposed species. The calculated phase diagrams show that the surfaces of InN and GaN can violate the electron counting rule. This is particularly the case for InN, where surfaces within the (2×2) symmetry under MOCVD conditions are mostly found to be conducting. It will be interesting to see whether the observed behavior holds under nonequilibrium conditions.

This work and use of Center for Nanoscale Materials (CNM) was supported by the US Department of Energy, Office of Science, Office of Basic Energy Sciences under Contract No. DE-AC02-06CH11357. We acknowledge grants of computer time from ANL Computing Resource Center (LCRC) and the National Energy Research Scientific Computing Center (NERSC).

*zapol@anl.gov

[1] A. G. Bhuiyan, A. Hashimoto, and A. Yamamoto, J. Appl. Phys. **94**, 2779 (2003).
[2] W. Walukiewicz *et al.*, J. Phys. D: Appl. Phys. **39**, R83 (2006).
[3] F. Jiang, A. Munkholm, R.-V. Wang, S. K. Streiffer, C. Thompson, P. H. Fuoss, K. Latifi, K. R. Elder, and G. B. Stephenson, Phys. Rev. Lett. **101**, 086102 (2008).
[4] O. Ambacher *et al.*, J. Vac. Sci. Technol. B **14**, 3532 (1996).
[5] C. G. Van de Walle and J. Neugebauer, Phys. Rev. Lett. **88**, 066103 (2002).
[6] C. G. Van de Walle and J. Neugebauer, J. Cryst. Growth **248**, 8 (2003).
[7] T. Ito, T. Nakamura, T. Akiyama, and K. Nakamura, Appl. Surf. Sci. **254**, 7659 (2008).
[8] S. Krukowski, P. Kempisty, and A. F. Jalbout, J. Chem. Phys. **129**, 234705 (2008).
[9] M. D. Pashley, Phys. Rev. B **40**, 10481 (1989).
[10] L. Zhang, E. G. Wang, Q. K. Xue, S. B. Zhang, and Z. Zhang, Phys. Rev. Lett. **97**, 126103 (2006).
[11] D. Segev and C. G. Van de Walle, Europhys. Lett. **76**, 305 (2005).
[12] V. Darakchieva *et al.*, Appl. Phys. Lett. **94**, 022109 (2009).
[13] P. D. C. King *et al.*, Phys. Rev. B **77**, 045316 (2008).
[14] V. Cimalla *et al.*, Appl. Phys. Lett. **89**, 172109 (2006).
[15] S. Limpijumnong and C. G. Van de Walle, Phys. Status Solidi B **228**, 303 (2001).
[16] D. C. Look *et al.*, Appl. Phys. Lett. **80**, 258 (2002).
[17] A. Janotti and C. G. Van de Walle, Appl. Phys. Lett. **92**, 032104 (2008).
[18] C. B. Duke, Chem. Rev. **96**, 1237 (1996).
[19] J. W. D. Connolly and A. R. Williams, Phys. Rev. B **27**, 5169 (1983).
[20] J. M. Sanchez, F. Ducastelle, and D. Gratias, Physica A **128**, 334 (1984).
[21] D. de Fontaine, *Solid State Physics* (Academic, New York, 1994), Vol. 47.
[22] H. Tang, A. Van der Ven, and B. L. Trout, Phys. Rev. B **70**, 045420 (2004).
[23] G. Kresse and J. Hafner, Phys. Rev. B **47**, R558 (1993); P. E. Blöchl, *ibid.* **50**, 17953 (1994).
[24] J. Heyd, G. E. Scuseria, and J. Ernzerhof, J. Chem. Phys. **118**, 8207 (2003).
[25] *CRC Handbook of Chemistry and Physics*, edited by David R. Lide, 73rd ed. (CRC Press, Boca Raton, Florida, 1992), p. 518.
[26] D. R. Stull and H. Prophet, *JANAF Thermochemical Tables*, 2nd ed., US National Bureau of Standards (US EPO, Washington, DC, 1971).
[27] M. R. Ranade, F. Tessier, A. Navrotsky, and R. Marchand, J. Mater. Res. **16**, 2824 (2001).
[28] H. Suzuki, R. Togashi, H. Murakami, Y. Kumagai, and A. Kouki, Jpn. J. Appl. Phys. **46**, 5112 (2007).
[29] J. Wu *et al.*, Appl. Phys. Lett. **80**, 3967 (2002).
[30] Y. Nanishi, Y. Saito, and T. Yamaguchi, Jpn. J. Appl. Phys. **42**, 2549 (2003).
[31] C. G. Van de Walle and D. Segev, J. Appl. Phys. **101**, 081704 (2007).
[32] A. Belabbes, J. Furthmüller, and F. Bechstedt, Phys. Rev. B **84**, 205304 (2011).
[33] H. Lu, W. J. Schaff, L. F. Eastman, and C. E. Stutz, Appl. Phys. Lett. **82**, 1736 (2003).
[34] L. F. J. Piper *et al.*, Appl. Phys. Lett. **88**, 252109 (2006).
[35] J. E. Northrup, J. Neugebauer, R. M. Feenstra, and A. R. Smith, Phys. Rev. B **61** 9932 (2000).